PHYSICAL REVIEW B **70**, 180402(R) (2004)

Tracking the local reversal processes in nanostructures by magnetic speckles

K. Chesnel,[1,2] M. Belakhovsky,[2] G. van der Laan,[3] F. Livet,[4] A. Marty,[2] G. Beutier,[2] S. P. Collins,[5] and A. Haznar[3,6]
[1]*ALS, Lawrence Berkeley National Laboratory, 1 Cyclotron Road, Berkeley, California 94720, USA*
[2]*DRFMC, CEA-Grenoble, 17 Avenue des Martyrs, 38054 Grenoble, France*
[3]*Magnetic Spectroscopy, Daresbury Laboratory, Warrington WA4 4AD, United Kingdom*
[4]*LTPCM, ENSEEG-Domaine Universitaire, BP 75, 38402 Saint-Martin d'Hères, France*
[5]*Diamond Light Source, Rutherford Appleton Laboratory, Didcot OX11 0QX, United Kingdom*
[6]*ILT&SR, Polish Academy Sciences, P.O. Box 1410, 50-950 Wroclaw 2, Poland*
(Received 16 July 2004; published 15 November 2004)

We have used coherent soft x-ray resonant magnetic scattering to locally track reversal processes in magnetic nanostructures. Coherent illumination of a limited number of nano-objects in a CoPt nanoline grating produces a specific speckle pattern, whose evolution under *in situ* magnetic field reveals the true local magnetic ordering. While each nanoline behaves as a single macrospin whose direction depends on the dipolar coupling with neighbors, the global reversal of the line array is successively governed by two effects: first, by the random distribution of defects, followed by the dipolar coupling favoring antiferromagnetic ordering.

DOI: 10.1103/PhysRevB.70.180402 PACS number(s): 75.75.+a, 75.25.+z, 75.60.Ej, 78.70.Ck

Burgeoning technological interest in perpendicular recording using nanostructured media has led to a strong incentive to study the basic properties of the underlying physical processes, such as the magnetization reversal. Photon in-photon out techniques are well suited to follow these processes in advanced materials, especially because *in situ* magnetic fields can be applied. The interaction between polarized photons and electrons in magnetic materials, extensively used in the visible region, is now starting to entrench in the x-ray region.[1–6] Soft x-ray resonant magnetic scattering (SXRMS) is a powerful tool to study magnetic media, providing vector magnetometry on a wavelength scale (1 nm–1 μm) that allows probing both the lateral and depth characteristic lengths of the magnetic ordering. In addition, use of coherent radiation would give information about the local magnetic configuration,[7,8] whereas classical (incoherent) scattering involves averaging over a bigger illuminated area. Recently, Pierce *et al.*[9] have used the coherent magnetic scattering technique as metrology to study the magnetic memory in thin continuous film. In their work they calculate the cross correlation between speckle patterns recorded at different points of the magnetization loop in order to quantify statistically the return point memory of the magnetic domains over the illuminated area. The value of this approach is that Pierce *et al.* were able to demonstrate a technique for extracting important information from x-ray speckle patterns without the need for reconstructing the real-space domain patterns—a highly complex process that has only been demonstrated in the most ideal of conditions. Here, we demonstrate a completely different technique, whereby magnetic information is obtained through a combination of speckle measurements and magnetic modeling. As shown by our coherent SXRMS results from a Co/Pt line array, where the reversal process has been monitored along the hysteresis curve, the implication is a true insight into the local processes.

The sample under study is a line grating etched into a silicon wafer and covered with a Co/Pt multilayer that exhibits perpendicular magnetization.[10,11] The patterned sample consists of 200-nm-wide lines separated by grooves 75-nm wide and 300-nm deep. The magnetic film deposited on the full wafer consists of a stacking of 13 [0.5-nm Co/1.8-nm Pt] bilayers. These geometrical parameters and growth conditions were chosen to give a uniform perpendicular magnetization across the full length of the lines.[12] Several SXRMS studies have been reported on perpendicularly magnetized CoPt thin films,[9,13,14] however, mainly concerning continuous films.

The use of coherent soft x rays provides a unique opportunity to go well beyond incoherent SXRMS results,[11] by following the local reversal mechanism: it has the potential

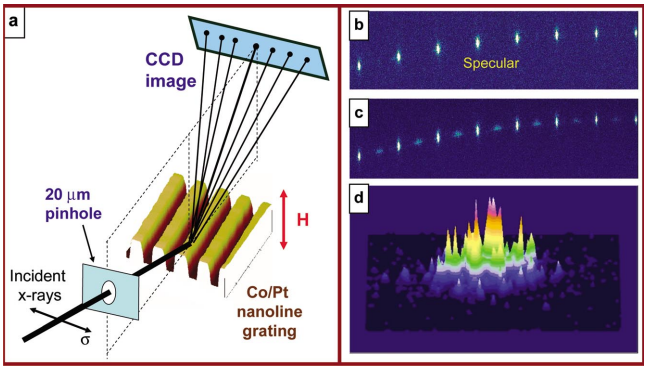

FIG. 1. (Color online) (a) Sketch of the experimental set up (not to scale) for coherent scattering in reflection geometry with an incidence angle θ=22.5°. The scattering pattern is recorded using a charge-coupled device (CCD) camera at 2θ=45°. Each line in the CoPt multilayer grating studied here can have either up or down magnetization. The CCD images of the coherent scattering pattern from the patterned sample in the initial demagnetized state (b) below the absorption edge, at 770 eV; (c) at the Co L_3 edge (780 eV) magnetic satellites appear between the structural diffraction peaks; (d) three-dimensional representation of the intensity fluctuations in the first magnetic satellite at the right-hand side of the specular peak.

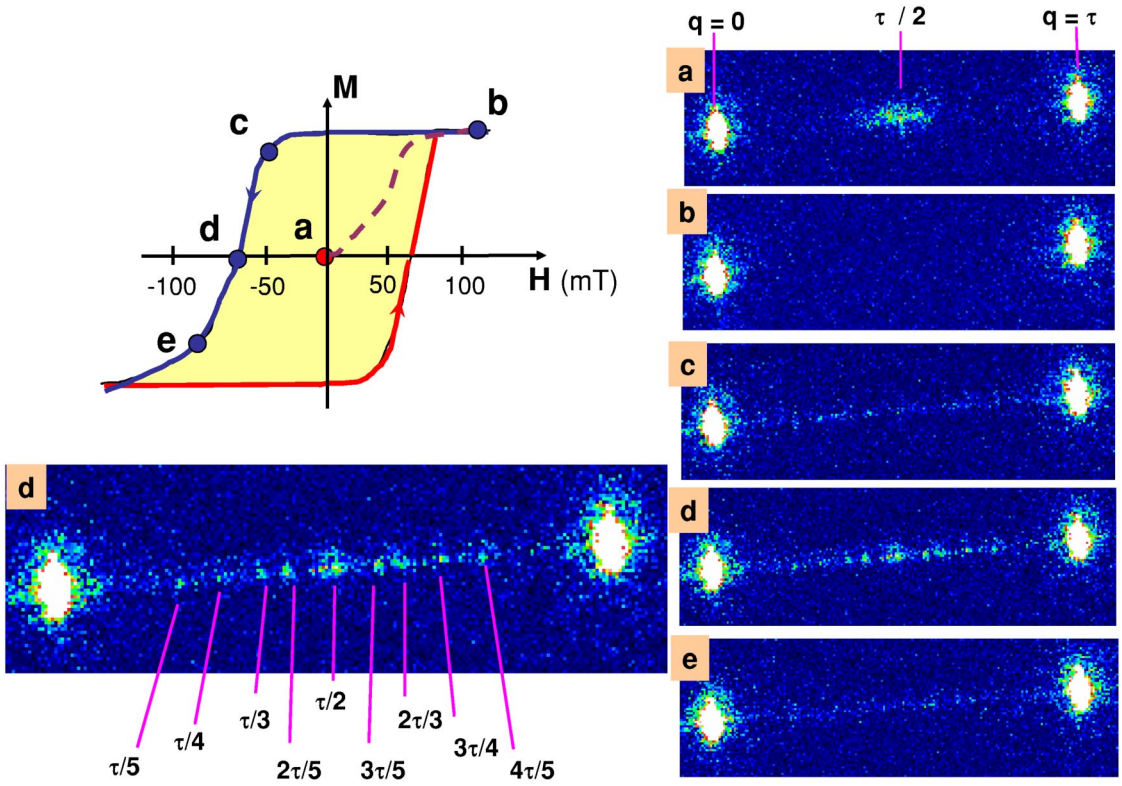

FIG. 2. (Color online) Evolution of the scattering pattern at various stages through the hysteresis loop: (a) initial demagnetized state ($H=0$); (b) positive saturation ($H=150$ mT); (c) apparent nucleation point ($H=-50$ mT); (d) coercive point ($H=-75$ mT); the positions of the most intense magnetic spots are indicated on the enlarged image at the bottom left, evidencing magnetic peaks at $\tau/2$, $\tau/3$, $\tau/4$, $\tau/5$, and their harmonics, corresponding to areas with different alternation periods up to $p=5$; (e) reversal end ($H=100$ mT). The images cover the region between the central specular spot ($q=0$) and first-order structural peak ($q=\tau$).

to give access to the local magnetic configuration of the line array, since the illuminated area contains a very limited number of nanolines ($\sim$80) and therefore to obtain the spin state of each individual line, at each stage of the reversal process. This scattering technique can be contrasted with magnetic force microscopy (MFM), which is sensitive to the stray fields and hence gives the view from above the sample surface, whereas x rays can penetrate the material in depth and give chemical and element selectivity. By tuning the energy to the core resonance the weak magnetic signal can be increased by orders of magnitude when the magnetic orbitals are directly involved in the electric-dipole transition, such as the $2p \rightarrow 3d$ excitation in first-row transition metals, in our case the Co L_3 edge at 780 eV. The presented results are obtained using linear σ polarization for the incident light, which gives $\sigma \rightarrow \pi$ scattering, where σ (π) is the polarization perpendicular (parallel) to the scattering plane. In this case, one probes the magnetization component along the direction of the scattered beam.

The measurements were performed at beamline ID08 of the European Synchrotron Radiation Facility (ESRF) in reflection geometry, as shown in Fig. 1(a), using the Daresbury in-vacuum diffractometer.[15,16] In order to optimize the scattering contrast in the speckle pattern, the beam requires a high degree of coherence, which was achieved using a 20-μm circular pinhole positioned at 5 cm in front of the sample. The diffraction pattern observed in the image from a charge-coupled device (CCD) camera reveals a series of very intense and sharp spots [Fig. 1(b)]. The central spot corresponds to the specular reflection, whereas the equidistantly spaced superlattice peaks on both sides originate from the periodicity of the line array. The peak separation agrees with the 275-nm structural period and the sharpness of the spots reveals the long-range consistency of the etched pattern. Tuning the photon energy to the Co L_3 edge results in the appearance of magnetic satellites between the structural spots [Fig. 1(c)]. Their positions reveal the existence of antiferromagnetic (AF)-ordered areas with a magnetic period twice the structural one. This image was recorded at the remanent point after demagnetization of the sample as described below. The coherent light induces strong intensity fluctuations within the magnetic spots, as shown in more detail in Fig. 1(d). We emphasize the excellent quality of this pattern showing, a magnetic speckle pattern from a magnetic patterned nanostructure. The limited number of illuminated objects is, here, a crucial aspect, inducing the intensity fluctuation in the scattering pattern, which are not visible using either incoherent light or with a much larger illuminated area, because of the signal averaging. The number of illuminated nanolines ($\sim$80 lines for a 20-μm pinhole) matches indeed the oversampling condition, as this is the same order, and even smaller, as the number of pixels ($\sim$170) separating two structural peaks on the CCD camera. Under such conditions one can expect to retrieve the true local configuration

of the line assembly at each stage of the magnetization loop.

By applying an *in situ* magnetic field perpendicular to the surface, one can follow the evolution of the magnetic speckle pattern through the entire hysteresis loop. By continuously sweeping the magnetic field, a movie was recorded, from which the images in Fig. 2 were extracted, with a region of interest that comprises the central specular spot ($q=0$) and the first-order structural satellite ($q=\tau$, corresponding to the grating period $p=2\pi/\tau$). These images correspond to the specific points (a)–(e) in the hysteresis curve. The initial state (a) [see also Fig. 1(c)] was obtained by a specific demagnetization procedure consisting of saturating the sample and then very slowly decreasing the field while rotating the sample. This procedure leads to nucleation of single domains along each line and favors an AF ordering, giving well-defined magnetic satellites between the structural peaks [Fig. 2(a)]. By applying a saturation field (b) one observes the disappearance of these satellites and all lines become magnetized in the same direction [ferromagnetic (F) order] with the magnetic period equal to the structural period. Following the evolution of the scattering pattern along the downward branch of the hysteresis curve, one observes the appearance of a magnetic signal at the macroscopic nucleation point (c). This signal gradually increases up to the coercive point (d) and then gradually decreases until the system is fully saturated in the opposite direction. These results demonstrate an important effect, related to the reversal process and magnetic ordering: in state (a) the intensity is concentrated around the AF position, because the demagnetization process reinforces the tendency for AF ordering, while in state (d) the magnetic signal spreads out nonuniformly between the structural peaks. In a major loop measurement, the lines reverse more randomly, at different places, with very short correlation length, thus producing a widespread distribution of the magnetic signal, in reciprocal space. However, the sharpness of the magnetic scattering signal in the vertical direction on the image reveals a very long correlation length in the longitudinal direction (i.e., along the lines).

These results evidence that the global reversal process occurs by switching almost entire single-domain lines (instead of by nucleation and propagation of small domains along the lines) and can be divided in two regimes. At the beginning of the reversal (c) some lines switch at random locations that are statistically far from each other, without any magnetic coupling, and reversal is governed essentially by the intrinsic defect distribution. This random localization of the initial reversed lines produces a specific scattering pattern with a fluctuating static distribution of the magnetic signal that spreads out over the entire line between the specular spot ($q=0$) and the structural satellite ($q=\tau$), as shown in Fig. 2(c). When the external field increases, more lines gradually switch to opposite direction and come closer to each other, enhancing the influence of the dipolar coupling, up to the coercive point (d), where half the lines are reversed. In this second regime, the reversal is governed mainly by minimization of the dipolar energy, favoring AF ordering. We emphasize here the competition between random distributed defects and magnetic coupling in the reversal process, producing a very specific coherent scattering pattern with a widely spread magnetic signal, contrary to a pure AF nucleation process, which would only induce a magnetic peak situated at $q=\tau/2$ with no signal elsewhere. The speckle pattern obtained at the coercive point evidences a series of intense peaks, distributed between $q=0$ and $q=\tau$. This ultimate coercive configuration results from a compromise between the initial random reversal stage and the following stage of dipolar energy minimization: there is clearly a tendency for AF order, but this tendency is too weak to order the whole system that still exhibits a short correlation length. In other words, the magnetic configuration at this point can be described as a juxtaposition of small areas with various ↑ and ↓ macrospin alternations, giving different magnetic periods. Nonetheless, the AF order remains in a certain way the prevailing order, corresponding to the central peak at $q=\tau/2$ (period of $p=2$ lines). The system also exhibits ↑↑↓ sequences with a period of $p=3$ lines, giving rise to peaks at $q=\tau/3$ and $2\tau/3$; and ↑↑↑↓ sequences with $p=4$ lines, lead-

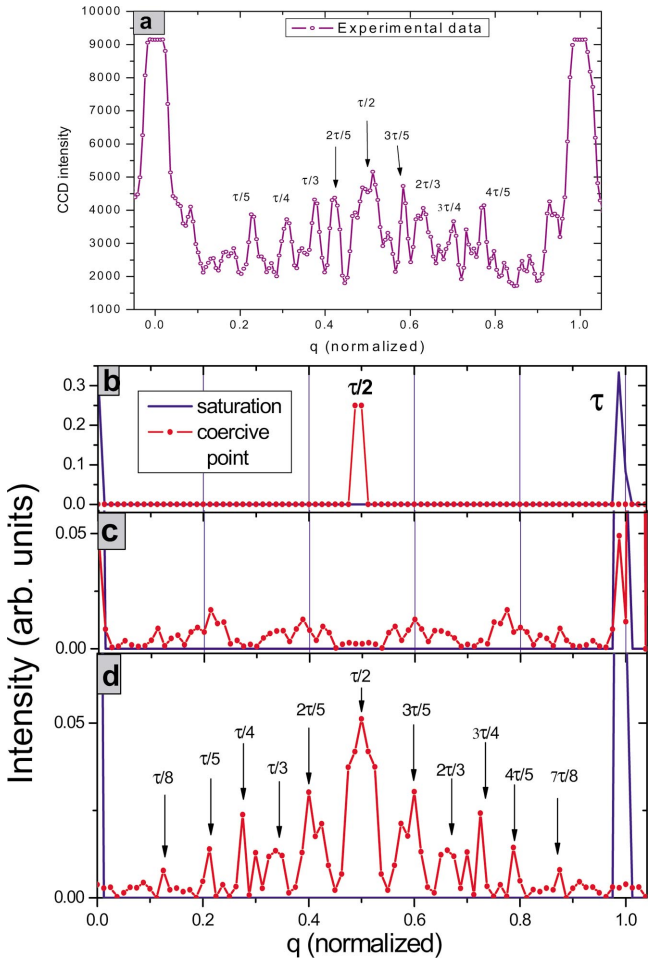

FIG. 3. (Color online) (a) Slice of the experimental CCD image at the coercive point [along the line in Fig. 2(d)]. The axis has been converted from pixel number to transversal scattering vector q, with normalization to $\tau=1$. The following plots represent simulation results for the pure magnetic part of the scattering intensity with $N=80$ lines for different reversal cases: (b) pure AF reversal, (c) random reversal; and (d) reversal driven by dipolar coupling between the lines. The drawn line corresponds to the initial state (saturation) and the lines with dots correspond to the coercive point where half of the nanolines is reversed.

ing to peaks at $q=\tau/4$, $\tau/2$, $3\tau/4$, etc. Beyond the coercive point the lines, that had not switched yet, reverse gradually and in a similar manner: first, due to dipolar coupling, thereafter, by random defect distribution, until the opposite saturation is completed.

In order to confirm the origin of the reversal process, we performed simulations of the magnetic scattering signal from an array of $N=80$ lines at different stages of the reversal. These one-dimensional (1D) simulations can be compared with an experimental slice of the CCD image measured at the coercive point [see Fig. 3(a)]. In the model, each line j is taken as a single domain carrying a normalized magnetization m_j that points either up (+1) or down (−1). The starting point is a saturation state, where all the lines are pointing up ($m_j=+1$ for all $j=1$ to N), then some specific lines switch from +1 to −1. Three different reversal modes have been considered, corresponding to three specific cases. The first case is the pure AF mode, where the AF ordering is producing a strong peak at $\tau/2$ as shown in Fig. 3(b); the second case is the purely random reversal mode, where the lines reverse at random location, thus producing in turn a random signal in reciprocal space as shown in Fig. 3(c). Finally, in the third mode, the dipolar interaction is taken into account and the first reversing lines are taken as far apart from each other as possible. This produces a superlattice structure corresponding to different periodicities as shown in Fig. 3(d). By comparing the results of these simulations to the experimental results, we can indeed conclude that the real reversal process is a mixture of these three theoretical modes: first, there is a tendency of random distribution of reversing lines mixed with reversal due to the dipolar coupling; then, after almost half of the lines are reversed (near the coercive point), a strong AF tendency appears, enhancing the central AF peak. A salient point is that we do not observe the satellites corresponding to rational wave vectors if we sample a large area (incoherent case), but only a broad AF central peak.[11] Therefore, the observation of the rational wave vectors is an important proof for the presence of local domain patterns.

In summary, our coherent SXRMS measurements demonstrate the feasibility to probe the true local magnetic configuration in nanostructures and its evolution under *in situ* fields. The remarkable changes of the speckle patterns obtained from a Co/Pt nanoline array along the hysteresis curve provide a precise fingerprint of the evolution of the magnetic domain configuration. The experimental results evidence that each Co/Pt line behaves like a macrospin that reverses completely above an intrinsic critical field. The whole reversal process can be divided into two regimes: the first stage is a random reversal phase, while the second stage is governed by the dipolar coupling favoring AF ordering. This analysis evidences two different regimes in the reversal process of the line assembly. The border between the two regimes depends on the pattern geometry, but also on the intrinsic reversal field distribution and can be modified by various parameters, such as layer deposition mode and magnetic history. The unprecedented quality of the observed speckle patterns are a prerequisite for the reconstruction in real space, in the longer term. Combined with the time structure of synchrotron radiation, these speckle patterns will enable us to study rapid fluctuations in the local magnetic order, giving access to dynamical processes, and ultimately leading to improvements in the read-write speed of magnetic storage devices.

We would like to thank J. Moritz and S. Landis for sample characterizations, M. D. Roper for the technical realizations, and S. S. Dhesi, P. Bencok, K. Larsson, and N. B. Brookes for their help on ESRF beamline ID08. Samples were fabricated at the CEA-Grenoble/LETI; diffractometer, magnets, and pinhole support were provided by SRS Daresbury; and CCD camera by ESRF.

[1] F. de Bergevin and M. Brunel, Phys. Lett. A **39**, 141 (1972).
[2] M. Blume, J. Appl. Phys. **57**, 3615 (1985).
[3] J. P. Hannon, G. T. Trammell, M. Blume, and D. Gibbs, Phys. Rev. Lett. **61**, 1245 (1988).
[4] D. Gibbs, J. Hill, and C. Vettier, Phys. Status Solidi B **215**, 667 (1999).
[5] H. A. Dürr, E. Dudzik, S. S. Dhesi, J. B. Goedkoop, G. van der Laan, M. Belakhovsky, C. Mocuta, A. Marty, and Y. Samson, Science **284**, 2166 (1999).
[6] N. Jaouen, J.-M. Tonnerre, D. Raoux, E. Bontempi, L. Ortega, M. Muenzenberg, W. Felsch, A. Rogalev, H. A. Dürr, E. Dudzik, G. van der Laan, H. Maruyama, and M. Suzuki, Phys. Rev. B **66**, 134420 (2002).
[7] J. F. Peters, M. A. de Vries, J. Miguel, O. Toulemonde, and J. B. Goedkoop, European Synchrotron Radiation Facility (ESRF) **32**, 12 (2000).
[8] B. Hu, P. Geissbuhler, L. Sorensen, S. D. Kevan, J. B. Kortright, and E. E. Fullerton, Synchrotron Radiat. News **14**(2), 17 (2001).
[9] M. S. Pierce, R. G. Moore, L. B. Sorensen, S. D. Kevan, O. Hellwig, E. E. Fullerton, and J. B. Kortright, Phys. Rev. Lett. **90**, 175502 (2003).
[10] S. Landis, B. Rodmacq, and B. Dieny, Phys. Rev. B **62**, 12271 (2000).
[11] K. Chesnel, M. Belakhovsky, S. Landis, J. C. Toussaint, S. P. Collins, G. van der Laan, E. Dudzik, and S. S. Dhesi, Phys. Rev. B **66**, 024435 (2002).
[12] K. Chesnel, M. Belakhovsky, S. Landis, B. Rodmacq, E. Dudzik, S. P. Collins, S. S. Dhesi, and G. van der Laan, IEEE Trans. Magn. **37**, 1661 (2001).
[13] J. B. Kortright, S.-K. Kim, G. P. Denbeaux, G. Zeltzer, K. Takano, and E. E. Fullerton, Phys. Rev. B **64**, 092401 (2001).
[14] O. Hellwig, S. Maat, J. B. Kortright, and E. E. Fullerton, Phys. Rev. B **65**, 144418 (2002).
[15] G. van der Laan, Synchrotron Radiat. News **14**(5), 32 (2001).
[16] K. Chesnel, M. Belakhovsky, F. Livet, S. P. Collins, G. van der Laan, S. S. Dhesi, J. P. Attané, and A. Marty, Phys. Rev. B **66**, 172404 (2002).